

## Article

# Effect of Pyrolysis Treatment on Phosphorus Migration and Transformation of Pig, Cow and Sheep Manure

Fen Liu <sup>1,2</sup>, Zhihua Xiao <sup>3,\*</sup>, Jun Fang <sup>1,2,\*</sup> and Hao Li <sup>1,2</sup>

<sup>1</sup> Hunan Engineering Laboratory for Pollution Control and Waste Utilization in Swine Production, Hunan Agricultural University, Changsha 410128, China; liufen1989@hunau.edu.cn (F.L.); lihao2001@stu.hunau.edu.cn (H.L.)

<sup>2</sup> College of Bioscience and Biotechnology, Hunan Agricultural University, Changsha 410128, China

<sup>3</sup> Key Laboratory for Rural Ecosystem Health in Dongting Lake Area of Hunan Province, Changsha 410128, China

\* Correspondence: xiaozhihua@hunau.edu.cn (Z.X.); fangjun1973@hunau.edu.cn (J.F.); Tel.: +86-731-84673603 (J.F.)

**Abstract:** Pig, cow, and sheep manure (PM, CM, and SM) are inevitable byproducts of agricultural economic development. Converting them into high add-on value biochar (PMB, CMB, and SMB) via pyrolysis is an efficient resource utilization measure. Phosphorus (P) speciation analyses help ensure the practical feasibility of the P reclamation of animal manure and their derived biochar and a reduction in environmental risk. This study conducted a modified extraction procedure to separate five inorganic P (IP) (soluble and loosely bound IP, aluminum-bound IP, Fe-bound IP, oxide-occluded IP, and Ca-bound IP) and organic P (OP) speciations, and combined X-ray diffraction (XRD) to investigate the major phosphate compound in the derived biochar after pyrolysis. Results revealed that more than 92% of P is concentrated in the derived biochar during pyrolysis processes carried out at 200–800 °C. The percentages of soluble and loosely bound IP, aluminum-bound IP, and OP in manure decreased significantly due to their transformation into more stable P fractions such as Ca-bound IP (79.01% in PMB, 800 °C) after pyrolysis. The Olsen-P percentages had a distinct reduction at 650 °C, indicating that pyrolysis at 650 °C was the optimal condition for the reduction in Olsen-P in manure.

**Keywords:** phosphorus; speciation; derived biochar; XRD; pyrolysis; manure



check for updates

**Citation:** Liu, F.; Xiao, Z.; Fang, J.; Li, H. Effect of Pyrolysis Treatment on Phosphorus Migration and Transformation of Pig, Cow and Sheep Manure. *Sustainability* **2023**, *15*, 9215. <https://doi.org/10.3390/su15129215>

Academic Editor: Luciano Cavani

Received: 4 May 2023

Revised: 4 June 2023

Accepted: 5 June 2023

Published: 7 June 2023



**Copyright:** © 2023 by the authors. Licensee MDPI, Basel, Switzerland. This article is an open access article distributed under the terms and conditions of the Creative Commons Attribution (CC BY) license (<https://creativecommons.org/licenses/by/4.0/>).

## 1. Introduction

In China, economic stimulation and population explosion imply a large demand for animal products. As a consequence, a quantity of livestock manure is generated annually [1]. Many harmful substances existed in livestock manure due to unhealthy feeding patterns, including heavy metals, antibiotics, pathogens, and so on [2]. Meanwhile, livestock manure is a biomass resource containing abundant phosphorus (P), nitrogen, potassium, and organic matter, and it is also frequently considered as a soil fertilizer [3]. The release of undisposed and incompletely processed manure can cause widespread environmental pollution, including water eutrophication and hypoxia [4], the breeding of mosquitoes as well as resource waste [5]. Dealing with manure is of great significance.

P is a necessary element and a non-renewable resource in agroecological systems [6]. The extraction of excessive rock phosphate, which is expected to be exhausted within 70–140 years, would create a tremendous burden on the future sustainable use of P [7]. The reuse and recovery of other P forms would relieve the pressure of P circulation. The total P loss into the environment has increased in China [8], and the main reason for this is the release of undisposed and incompletely processed manure into water bodies [9]. The P release rate in livestock manure as a fertilizer is rapid (the release rate of the total content can reach up to 25%), exceeding soil retention capacity and plant needs [7,10]. Therefore,

there is increased interest in obtaining efficient P recycling from animal manure by means of treatment technologies.

Recently, numerous technologies have been developed for the treatment of livestock manure in order to efficiently recycle P, and these technologies include pyrolysis [7,11–13], composting [5,9], freeze–thaw cycles [14], electrocoagulation [15], and so on. Pyrolysis is commonly used for maximizing biochar production. Biochar plays an important role in environmental remediation [16,17], and it has been reported that the biochar derived from municipal sewage sludge, rice straw, and distiller grains contains more stable P after carbonization for recycling processes [18,19]. The mobility and bio-availability of P in an ecological environment are closely related to its speciation; therefore, it is extremely necessary to study the P speciation characterization of biochar. Chu et al. [20] studied pyrogenic and modified carbon properties via pyrolysis and the phosphoric-acid-assisted pyrolysis of lignocellulose at 200 °C to 500 °C. It was observed that the soluble P concentration decreased with an increase in temperature during phosphoric-acid-assisted pyrolysis. Adhikari et al. [7] found that the available P transformed into a less available pool after the pyrolysis of biosolids at 400 °C to 600 °C. Li et al. [21] explored P speciation in sewage sludge and its biochar using a solution and 28 solid-state P nuclear magnetic resonance and X-ray diffraction (XRD) instances; the results revealed that inorganic orthophosphates are the predominant molecular configurations after pyrolysis. Similar results were found by Zhu et al. [22] who disposed of sewage sludge by carrying out pyrolysis. However, research studies on P speciation transformation during the pyrolysis of manure have seldom been reported.

Pig manure, cow manure, and sheep manure are typical livestock manure and biomass resources. This study disposed of these three manure types by carrying out pyrolysis. The purposes of this study are as follows: (1) quantify the total P content to estimate the mass balance of P after pyrolysis; (2) characterize P speciation in these three raw materials and their derived biochar systematically to clarify the mechanism of P transformation and migration; (3) determine the main phosphates characteristics via XRD to analyze stable p crystalline substances in biochar after pyrolysis. From the perspective of sustainable development, this study contributes to the recycling of P and biomass resources in ecological environments.

## 2. Materials and Methods

### 2.1. Sample Collection

Pig manure (PM) was collected from a massive industrial pig farm on the outskirts of Changsha City, Hunan Province, resulting in high P concentrations of PM. Primarily finishing pigs, little partly sows and piglings were raised on the farm. Cow manure (CM) was gathered from a small farm in Ningxiang City, and sheep manure (SM) was gathered from farmers in Ningxiang City, Hunan Province. The sheep were raised using scatter-feed methods without adding animal feed additives.

Fresh PM, CM, and SM were desiccated in a furnace at 60 °C for 3 days. The desiccated samples were mechanically ground in a grinding ball mill and sieved via a 0.18 mm mesh. The elemental compositions of the three types of manure were determined via an elemental analyzer (Vario EL III, German). Proximate analysis was carried out on solid biofuels (GB/T28731-2012) via a muffle furnace. The results of elemental, proximate, and fiber analyses of the manure are shown in Table 1.

**Table 1.** Properties of pig manure (PM), cattle manure (CM), and sheep manure (SM).

Properties	Pig Manure	Cattle Manure	Sheep Manure
Elemental analysis <sup>a</sup> (wt %)			
C	33.51 ± 0.44	37.96 ± 0.20	38.74 ± 0.27
H	5.72 ± 0.04	5.65 ± 0.05	5.24 ± 0.07
O	57.48 ± 0.42	54.14 ± 0.17	53.65 ± 0.28
N	3.06 ± 0.07	2.17 ± 0.06	2.31 ± 0.06
S	0.23 ± 0.02	0.08 ± 0.01	0.06 ± 0.01
P	2.08 ± 0.09	1.37 ± 0.04	0.80 ± 0.03
Proximate analysis <sup>b</sup> (wt %)			
Moisture	6.61 ± 0.05	7.49 ± 0.08	6.34 ± 0.10
Ash	32.43 ± 0.25	22.63 ± 0.19	27.39 ± 0.20
Volatile matter	54.52 ± 0.28	54.95 ± 0.43	55.48 ± 0.36
Fixed carbon	6.44 ± 0.14	14.93 ± 0.18	10.79 ± 0.11
Fiber analysis <sup>a</sup> (wt %)			
Hemicelluloses	20.23 ± 0.11	21.51 ± 0.14	16.87 ± 0.05
Cellulose	8.03 ± 0.04	18.05 ± 0.11	11.57 ± 0.08
Lignin	9.09 ± 0.06	14.48 ± 0.07	21.88 ± 0.18

<sup>a</sup> Dry matter basis. <sup>b</sup> As received. Data was reported as mean value ± standard deviation.

## 2.2. Preparation of Biochar Samples

The pyrolysis reactor is a horizontal and lab-scale tubular furnace (SK-G08123K, China). The reactor contains a gas supply, an electrical heater, a programmable temperature controller, and a tubular unit. Pyrolysis chars were produced by the pyrolysis of PM, CM, and SM, heating these samples in an oxygen-limited atmosphere at 200, 350, 500, 650, and 800 °C.

In each pyrolysis operation, pulverized PM, CM, and SM (10 g) were packed into ceramic crucibles. The manure was heated up to the final reaction temperatures at a rate of 10 °C/min; pure nitrogen flow at 200 mL/min as the carrier gas was used during pyrolysis operations. The produced pyrolysis biochar of PM, CM, and SM at 200, 350, 500, 650, and 800 °C were labeled PMB (PMB200, PMB350, PMB500, PMB650, and PMB800), CMB (CMB200, CMB350, CMB500, CMB650, and CMB800) and SMB (SMB200, SMB350, SMB500, SMB650, and SMB800) according to their samples and carbonization temperature. The obtained biochar was naturally cooled to room temperature in a desiccator, ground using a ceramic mortar and pestle, and sieved with 100 meshes (150 µm). The ground samples were stored in plastic bags in a desiccator before being transported to the laboratory for the determination of P.

## 2.3. Separation of Different P Fractionations

The total P (TP) and inorganic P (IP) concentrations were analyzed via the ignition approach [23]. TP content was analyzed by igniting 1.0 g of manure or biochar at 550 °C for 1 h, and then extractions using 25 mL of 0.5 mol L<sup>-1</sup> sulfuric acid were carried out for 2 h. IP concentration was determined using the same extraction routine. The two liquid–solid phases were sieved, and centrifugation was carried out at 4000 rpm for 20 min. Next, the supernatant was sieved via a 0.45 µm filter. TP and IP concentrations were determined using the molybdenum blue approach [24]. The organic P (OP) concentration was determined as the difference between TP and IP. Then, the IP fractions in manure and biochar were separated into soluble and loosely bound IP (SL-IP), aluminum-bound IP (Al-IP), Fe-bound IP (Fe-IP), oxide-occluded IP (O-IP), and Ca-bound IP (Ca-IP) using agrochemical soil analysis methods, and the specific experimental process was carried out as follows.

Step 1: SL-IP. Samples (1.0 g) were imported into 100 mL centrifugal tubes containing 50 mL of 1.0 mol L<sup>-1</sup> ammonium chloride and shaken for 30 min at 25 °C. The two liquid–solid phases were sieved, and centrifugal separation was carried out at 3500 rpm for 8 min.

Then, the supernatant was filtered via a 0.45  $\mu\text{m}$  membrane filter. The residual solid was retained for follow-up extractions.

Step 2: Al-IP. During this step, a 50 mL volume of 0.5 mol L<sup>-1</sup> ammonium fluoride (pH = 8.2) was added to the residual solid obtained from step 1 in a centrifugal tube, which was shaken for 1 h at 25 °C. The extraction procedure described above was followed.

Step 3: Fe-IP. During this step, a 50 mL volume of 0.1 mol L<sup>-1</sup> sodium hydroxide was added to the residue obtained from step 2. The mixed solid–liquid was shaken for 2 h, stood for 1 h, and then shaken for 2 h at 25 °C. The two liquid–solid phases were separated via centrifugal separation at 4500 rpm for 10 min. Then, the supernatant was sieved via a 0.45  $\mu\text{m}$  filter. Moreover, 1.5 mL of concentrated sulfuric acid (98%) was added to the solution. The residual solid was retained for follow-up extractions.

Step 4: O-IP. The residue from step 3 was shaken at 90 °C in a water bath for 15 min with 40 mL of 0.3 mol L<sup>-1</sup> Na<sub>3</sub>C<sub>6</sub>H<sub>5</sub>O<sub>7</sub> and 1.0 g of sodium hydrosulfite. Subsequently, 10 mL of 0.5 mol L<sup>-1</sup> sodium hydroxide was added, and the compound was stirred again at 90 °C in a water bath for 10 min. Finally, the extract was obtained after following the procedure described in step 3.

Step 5: Ca-IP. The residue from the fourth step was shaken at 25 °C for 1 h with 50 mL of 0.25 mol L<sup>-1</sup> H<sub>2</sub>SO<sub>4</sub>.

The supernatant liquids obtained from steps 1, 2, 3, 4, and 5 were all then sieved via a 0.45  $\mu\text{m}$  filter. All experiments were carried out in quadruplicate.

#### 2.4. Olsen-P

The Olsen-P (available soil P) content can be indicated via the availability of P (especially IP, although it contains a small quantity of OP) in calcareous soils; it was measured by applying the molybdenum blue method after extraction by NaHCO<sub>3</sub> (0.5 mol L<sup>-1</sup>, pH = 8.5) [25].

#### 2.5. P Determination

TP and various IP concentrations were tested with a UV-visible spectrophotometer at a specific wavelength (880 nm). The main mineral phases of raw materials and the derived biochar were measured via XRD. Then, XRD analyses were carried out via a D8 ADVANCE powder X-ray diffractometer using MDI Jade 6.0 software.

#### 2.6. Residual Rate

The residual rate is defined as the ratio of the total quantity of P in biochar to that in manure. According to the yields of PMB, CMB, and SMB during the pyrolysis process and TP in manure and biochar, the value of residual rates can be calculated using the following formula:

$$\text{Residual rate (\%)} = \frac{\text{TPB} \times \text{Y}}{\text{TPM}} \times 100$$

where TPB represents the total concentration of P in biochar (mg kg<sup>-1</sup>); Y is the yield of biochar in the pyrolysis experiment; TPM represents the total concentration of P in material (mg kg<sup>-1</sup>).

#### 2.7. Statistical Analysis

The consequences were evaluated statistically using SPSS 19.0 software. All results were tested for normal distribution (Shapiro–Wilk's test) and homogeneity of variance (Levene's test). After performing one-way ANOVA, Tukey's tests ( $p < 0.05$ ) were carried out to spot significant differences among materials and the derived biochars within the same material. Simultaneously, the consequences were obtained as mean value  $\pm$  standard deviation (SD) ( $n = 4$ ) in this research study.

### 3. Results and Discussion

#### 3.1. Mass Balance of P

The total contents of P in manure and biochar are listed in Table 2. The concentrations of P in manure samples are reflected in the following order: SM < CM < PM. The concentration range of the examined manure ranged from 7.96 mg g<sup>-1</sup> (SM) to 20.76 mg g<sup>-1</sup> (PM). In this study, the P total content of PM and CM was similar to previously reported values, and studies found that the average total content of P ranged from 15.80 mg/g to 18.2 mg/g [26] separately in PM and 5.8 to 9.1 mg/g [27] in SM. Inorganic phosphates (for example, dicalcium phosphate and monocalcium phosphate) have been generally used in cow and pig diets as complementary P sources to compensate for the low bioavailability of P in fodder [28]. They may be responsible for the high P concentrations of PM and CM. The sheep were raised using scatter-feed methods without adding animal feed additives, resulting in low P concentrations of SM.

**Table 2.** Contents of phosphorus in dried manure and biochar and the residual rate of phosphorus in biochar.

Temperature	Pig Manure		Cow Manure		Sheep Manure	
	Contents (mg g <sup>-1</sup> )	Ratios (%)	Contents (mg g <sup>-1</sup> )	Ratios (%)	Contents (mg g <sup>-1</sup> )	Ratios (%)
Material	20.76 ± 0.87 <sup>d</sup>		13.72 ± 0.44 <sup>d</sup>		7.96 ± 0.33 <sup>d</sup>	
Biochar 200	23.34 ± 0.39 <sup>c</sup>	98.44	15.58 ± 0.61 <sup>c</sup>	97.54	8.88 ± 0.54 <sup>d</sup>	96.94
Biochar 350	37.48 ± 0.52 <sup>b</sup>	98.71	26.49 ± 0.56 <sup>b</sup>	98.26	13.89 ± 0.38 <sup>c</sup>	97.92
Biochar 500	43.12 ± 0.94 <sup>a</sup>	97.20	29.41 ± 0.73 <sup>b</sup>	96.02	15.97 ± 0.64 <sup>b</sup>	97.67
Biochar 650	44.81 ± 0.85 <sup>a</sup>	97.35	32.26 ± 0.97 <sup>a</sup>	97.26	17.42 ± 0.52 <sup>a</sup>	94.76
Biochar 800	44.54 ± 1.02 <sup>a</sup>	92.14	32.48 ± 0.69 <sup>a</sup>	94.90	17.91 ± 0.81 <sup>a</sup>	92.46

Each trial was carried out in quadruplicate. Data was reported as mean value ± SD. Different lowercase letters indicate significance ( $p < 0.05$ , Tukey's test) among materials and the derived biochar within the same material.

As shown in Table 2, the contents of P increased in the biochar, with the exception of PMB800 due to increasing pyrolysis temperatures. It was easily observed that the total P content more than doubled in the derived biochar when the pyrolysis temperature exceeded 500 °C. This is due to high pyrolysis temperatures, causing the decomposition and volatilization of organic matter in manure. The residual rate of P in the biochar can be a great indicator for studying the transformation behavior of P during pyrolysis. Contrary to the total content of P, as pyrolysis temperatures increased, the residual ratio of P slightly decreased. It was shown that within a pyrolysis temperature range of 200–800 °C, more than 92% of P in the biochar was retained, indicating that most P remained in the biochar. Many phosphorous compounds possessed high melting points, and these include the melting points of Na<sub>3</sub>PO<sub>4</sub>, Ca<sub>10</sub>(PO<sub>4</sub>)<sub>6</sub>(OH)<sub>2</sub>, and Ca<sub>3</sub>(PO<sub>4</sub>)<sub>2</sub>, which exceeded 1545 °C, 1650 °C, and 1670 °C, respectively; this may be account for the high residual rate of P [29].

#### 3.2. P Speciation

It is well known that TP cannot supply information on the nature of P chemical forms; thus, P fractionation should be presented in research studies for it can provide a method for investigating the bioavailability, solubility, and interconversion of P fractions. The bioavailability of P fractions reflects the following sequence: SL-IP > Al-IP > Fe-IP > O-IP > Ca-IP; this is consistent with the order of inorganic P dissolvability and in accordance with the inorganic P fractionation scheme [25]. From Table 3, the recovery rates of P ranged from 91.89% to 106.54%, showing that the emendatory sequential extraction method applied to surveying the speciation concentrations of P in raw materials and derived biochar was exact and reliable.

**Table 3.** Total concentration and speciation of phosphorus ( $\text{mg g}^{-1}$ ).

Biochar	SL-IP	Al-IP	Fe-IP	O-IP	Ca-IP	OP	Total	Recovery (%)
PM	5.88 ± 0.21 <sup>b</sup>	7.40 ± 0.31 <sup>a</sup>	0.45 ± 0.07 <sup>d</sup>	0.74 ± 0.05 <sup>f</sup>	0.16 ± 0.05 <sup>e</sup>	6.25 ± 0.32 <sup>b</sup>	20.76 ± 0.87 <sup>d</sup>	100.53
PM 200	5.72 ± 0.17 <sup>b</sup>	6.68 ± 0.18 <sup>b</sup>	0.32 ± 0.03 <sup>d</sup>	1.74 ± 0.04 <sup>e</sup>	0.37 ± 0.03 <sup>e</sup>	7.17 ± 0.33 <sup>a</sup>	23.34 ± 0.39 <sup>c</sup>	94.26
PM 350	7.68 ± 0.37 <sup>a</sup>	4.17 ± 0.23 <sup>d</sup>	1.93 ± 0.10 <sup>b</sup>	3.99 ± 0.18 <sup>d</sup>	14.04 ± 0.44 <sup>d</sup>	2.99 ± 0.26 <sup>c</sup>	37.48 ± 0.52 <sup>b</sup>	92.83
PM 500	3.41 ± 0.19 <sup>c</sup>	5.10 ± 0.38 <sup>c</sup>	2.62 ± 0.19 <sup>a</sup>	8.79 ± 0.25 <sup>a</sup>	19.60 ± 0.61 <sup>c</sup>	1.56 ± 0.11 <sup>d</sup>	43.12 ± 0.94 <sup>a</sup>	95.26
PM 650	1.40 ± 0.15 <sup>d</sup>	1.79 ± 0.17 <sup>e</sup>	0.73 ± 0.11 <sup>c</sup>	6.58 ± 0.32 <sup>b</sup>	32.09 ± 0.59 <sup>b</sup>	1.44 ± 0.12 <sup>d</sup>	44.81 ± 0.85 <sup>a</sup>	98.27
PM 800	0.92 ± 0.11 <sup>d</sup>	1.70 ± 0.11 <sup>e</sup>	0.74 ± 0.09 <sup>c</sup>	4.84 ± 0.18 <sup>c</sup>	35.85 ± 0.81 <sup>a</sup>	1.30 ± 0.11 <sup>d</sup>	44.54 ± 1.02 <sup>a</sup>	101.83
CM	7.92 ± 0.12 <sup>a</sup>	2.68 ± 0.17 <sup>c</sup>	0.40 ± 0.08 <sup>d</sup>	0.21 ± 0.04 <sup>e</sup>	0.02 ± 0.01 <sup>d</sup>	2.19 ± 0.11 <sup>b</sup>	13.72 ± 0.44 <sup>d</sup>	97.82
CM 200	8.32 ± 0.21 <sup>a</sup>	2.73 ± 0.15 <sup>c</sup>	0.70 ± 0.05 <sup>d</sup>	0.38 ± 0.05 <sup>e</sup>	0.06 ± 0.02 <sup>d</sup>	2.35 ± 0.15 <sup>ab</sup>	15.58 ± 0.61 <sup>c</sup>	93.35
CM 350	5.80 ± 0.23 <sup>b</sup>	4.85 ± 0.29 <sup>b</sup>	2.88 ± 0.24 <sup>c</sup>	4.97 ± 0.26 <sup>c</sup>	3.51 ± 0.29 <sup>c</sup>	2.59 ± 0.22 <sup>a</sup>	26.49 ± 0.56 <sup>b</sup>	92.83
CM 500	5.44 ± 0.27 <sup>b</sup>	6.72 ± 0.16 <sup>a</sup>	4.19 ± 0.36 <sup>b</sup>	5.96 ± 0.15 <sup>b</sup>	4.08 ± 0.18 <sup>c</sup>	1.05 ± 0.15 <sup>c</sup>	29.41 ± 0.73 <sup>b</sup>	93.28
CM 650	3.90 ± 0.14 <sup>c</sup>	6.51 ± 0.43 <sup>a</sup>	5.60 ± 0.39 <sup>a</sup>	7.00 ± 0.27 <sup>a</sup>	6.32 ± 0.40 <sup>b</sup>	0.98 ± 0.15 <sup>c</sup>	32.26 ± 0.97 <sup>a</sup>	93.93
CM 800	3.90 ± 0.14 <sup>c</sup>	5.17 ± 0.23 <sup>b</sup>	4.99 ± 0.40 <sup>a</sup>	1.74 ± 0.20 <sup>d</sup>	13.47 ± 0.46 <sup>a</sup>	0.58 ± 0.12 <sup>d</sup>	32.48 ± 0.69 <sup>a</sup>	91.89
SM	3.65 ± 0.14 <sup>a</sup>	1.03 ± 0.12 <sup>c</sup>	0.01 ± 0.01 <sup>c</sup>	0.80 ± 0.09 <sup>d</sup>	0.04 ± 0.01 <sup>e</sup>	2.72 ± 0.09 <sup>b</sup>	7.96 ± 0.33 <sup>d</sup>	103.54
SM 200	3.85 ± 0.13 <sup>a</sup>	0.98 ± 0.07 <sup>c</sup>	0.07 ± 0.03 <sup>c</sup>	1.44 ± 0.13 <sup>c</sup>	0.13 ± 0.02 <sup>e</sup>	2.99 ± 0.11 <sup>a</sup>	8.88 ± 0.54 <sup>d</sup>	106.54
SM 350	3.28 ± 0.19 <sup>b</sup>	3.01 ± 0.17 <sup>b</sup>	1.47 ± 0.11 <sup>a</sup>	2.41 ± 0.14 <sup>b</sup>	2.19 ± 0.14 <sup>d</sup>	1.15 ± 0.08 <sup>c</sup>	13.89 ± 0.38 <sup>c</sup>	97.30
SM 500	2.95 ± 0.26 <sup>b</sup>	4.62 ± 0.24 <sup>a</sup>	1.20 ± 0.13 <sup>b</sup>	3.23 ± 0.20 <sup>a</sup>	3.30 ± 0.21 <sup>c</sup>	0.92 ± 0.06 <sup>d</sup>	15.97 ± 0.64 <sup>b</sup>	101.58
SM 650	0.94 ± 0.10 <sup>c</sup>	1.19 ± 0.05 <sup>c</sup>	0.20 ± 0.03 <sup>c</sup>	3.21 ± 0.24 <sup>a</sup>	9.93 ± 0.18 <sup>b</sup>	0.85 ± 0.12 <sup>d</sup>	17.42 ± 0.52 <sup>a</sup>	93.72
SM 800	0.61 ± 0.09 <sup>c</sup>	1.32 ± 0.07 <sup>c</sup>	0.16 ± 0.05 <sup>c</sup>	2.46 ± 0.14 <sup>b</sup>	11.64 ± 0.28 <sup>a</sup>	0.84 ± 0.05 <sup>d</sup>	17.91 ± 0.81 <sup>a</sup>	95.02

Recovery = (SL-IP + AL-IP + Fe-IP + O-IP + Ca-IP + OP)/Total × 100. Date was reported as mean value ± SD. Different lowercase letters indicate a significant ( $p < 0.05$ , Tukey's test) among material and its derived biochars within the same material.

### 3.2.1. SL-IP

The concentrations and percentages of SL-IP in the manure and biochar were determined, and the results are shown in Table 3 and Figure 1A. As the TP concentrations in manure and their derived biochar are not the same, the quantities of SL-IP were normalized to the percentages of SL-IP in different samples. The high percentages of SL-IP in PM (28.09%), CM (59.2%), and SM (43.49%) were notable (Figure 1A). SL-IP represents a highly bioavailable P fraction [30,31]. Monocalcium phosphate ( $\text{Ca}(\text{H}_2\text{PO}_4)_2$ ), as a type of SL-IP, is a water-soluble phosphate (solubility is  $139.5 \text{ g L}^{-1}$ ) [32], and it is readily dissolved in soil liquids and highly effective in crop uptake [33]. Therefore, monocalcium phosphate is known as a high-quality fertilizer and has normally been used in cow and pig diets; it is responsible for the high percentages of SL-IP in manure. The form of water-soluble P in livestock manure may be more propitious for leaching processes that occur in fields and surface water; it can generate more poisonous impacts [34]. Meanwhile, the results also showed that an intense reduction happened in the SL-IP fractions after the transformation of manure into biochar via pyrolysis. With increasing pyrolysis temperatures, the percentages of SL-IP in all biochar types decreased, and a decrease occurred with respect to the concentrations of SL-IP in the biochar with the exception of PM 350, CM 200, and SM 200. Similar results could be reported by Qian and Jiang [35]. The pyrolysis treatment of manure substantially reduced SL-IP, which implied that pyrolysis could stabilize P in biochar, and the risk of potential P loss is reduced.

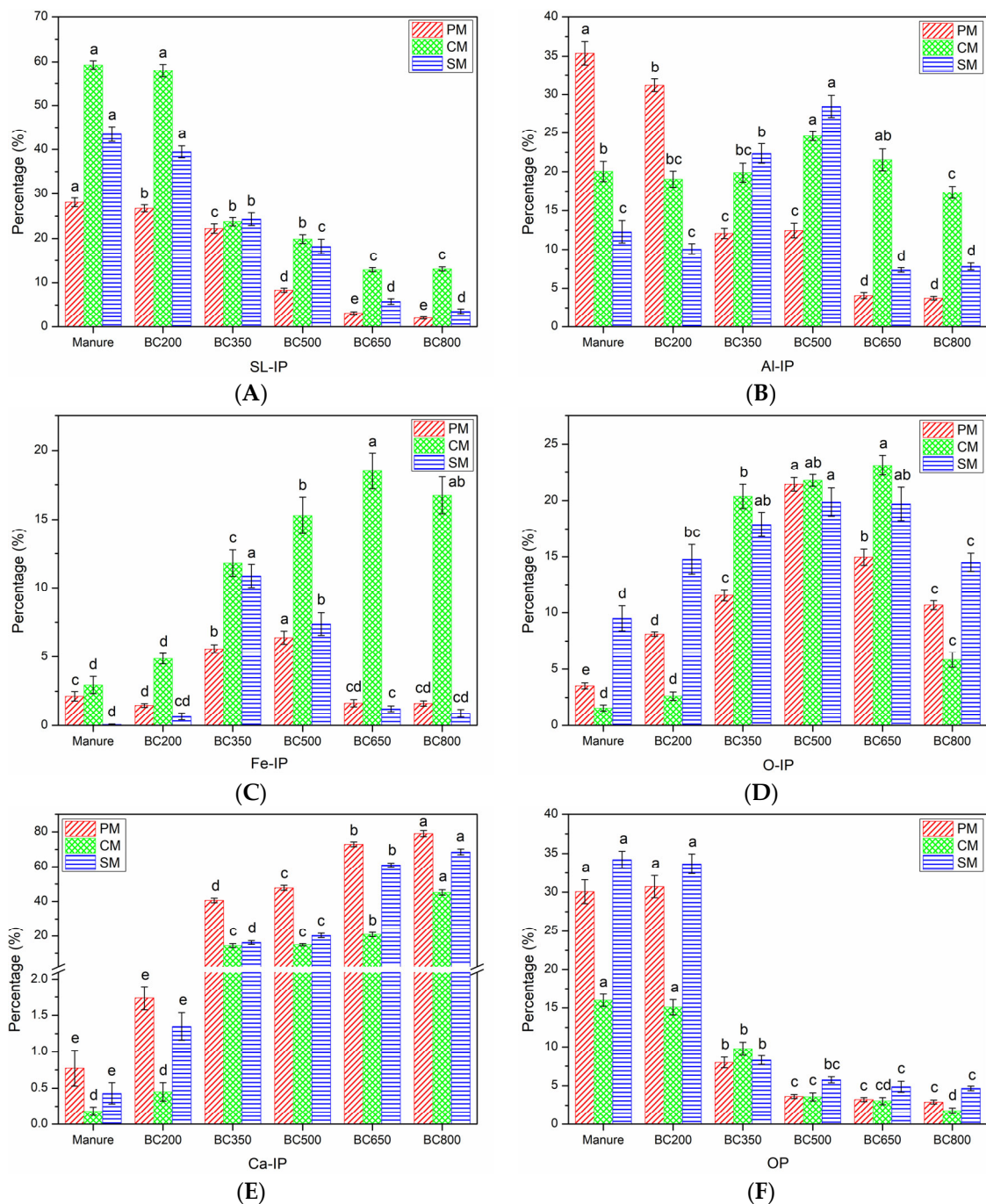


**Figure 1.** Speciation percentages of P in manure and the derived biochar. Bars with different lowercase letters indicate a significant difference ( $p < 0.05$ , Tukey's test) between materials and the derived biochar within the same material. Error bar represents a standard deviation ( $n = 4$ ). Percentages of (A) SL-IP, (B) Al-IP, (C) Fe-IP, (D) O-IP, (E) Ca-IP and (F) OP speciations in manure and the derived biochar.

### 3.2.2. AL-IP

Al-IP and SL-IP are both highly bioavailable P fractions [36]. The percentages of Al-IP are shown in Figure 1B. The figure reveals that the percentage of Al-IP in PM (35.38%) was markedly higher than those in CM (20.04%) and SM (12.29%). At the same time, Figure 1B shows that the percentages of Al-IP in PMB decreased with an increase in pyrolysis temperatures, indicating the Al-IP in PM may be stabilized in more steady P fractions during the process of the pyrolysis of PM. In other words, the increase in the

weight of Al-IP was lower than the loss in the weight of Al-IP during the pyrolysis of PM. Moreover, in CMB and SMB, an increase (200 °C to 500 °C) and then a decrease (500 °C to 800 °C) were detected in Al-IP's percentage, which suggested that SL-IP and OP were possibly transformed into Al-IP after the pyrolysis (temperatures beyond 500 °C) of CM and SM. In addition, the Al-IP fractions of the biochar (650 °C and 800 °C) were eventually lower than the fractions in their material, which demonstrated that charring organic waste decreased the quantity of the mobilizable P pool.

### 3.2.3. Fe-IP

The Fe-IP fraction was usually accepted in reductive conditions, where  $\text{Fe}^{3+}$  was readily reduced to  $\text{Fe}^{2+}$ , causing a release of Fe-IP [37]. Fe-IP was mobilizable in lake sediments, and it was responsible for an increase in eutrophication [38]. The results of the pyrolysis process that changed the percentages of Fe-IP are shown in Figure 1C. Compared to PM, the percentages of Fe-IP in PMB increased from 1.48% to 6.38% at 200–500 °C, and then they drastically decreased from 6.38% to 1.64% at 500–650 °C. Similar trends were observed in CMB and SMB, but the peak percentages of Fe-IP in CMB was CMB650 and that in SMB was SMB350. After the highest percentage was reached, there was an obvious drop off in Fe-IP content at the next temperature increment, especially in PMB and SMB. These results may be attributed to the observation that orthophosphates in the three manure types experienced dehydration or were polymerized at relatively low pyrolysis reaction temperatures; in contrast, this chemical progress was restrained at relatively high temperatures because of the formation of more stable phosphate crystals between various phosphate and metal ions, such as calcium phosphate crystal [35]. The peaks of the percentages of Fe-IP in the three manure types appeared at different reaction temperatures, and this observation may be related to the properties and heavy metal contents of manure.

### 3.2.4. O-IP

O-IP is considered a stable P speciation in soils and sediments, and it does not easily change and exhibits low bioavailability [14]. Compared to the changing trend of Fe-IP's percentage in biochar after pyrolysis with an increase in temperature, a similar result appeared in O-IP. From Figure 1D, in comparison with raw materials, it was revealed that the percentages of O-IP in PMB and SMB increased by 17.9% and 10.36% at 200–500 °C and then decreased by 10.75% and 5.38% at 500–800 °C, respectively. The percentages of O-IP in CMB also peaked at 23.14% at 650 °C. All above observations indicated that it was beneficial to move available P toward O-IP when pyrolysis temperatures increased beyond 650 °C.

### 3.2.5. Ca-IP

Ca-IP was a relatively non-bioavailable, inert, and stable P fraction. There may be substantial phosphate-solubilizing bacteria that can transform insoluble phosphate into bioavailable forms (SL-IP and Al-IP) [36]. As shown in Table 3 and Figure 1E, it was observed that the concentrations and percentages of Ca-IP increased with an increase in heating treatment temperatures in all biochar types. The percentages of Ca-IP significantly elevated from 0.77% to 79.01%, from 0.18% to 45.22%, and from 0.43% to 68.54% in PMB, CMB, and SMB, respectively, after the three manure types were heated at 800 °C. This experimental result might be explained by the transformation of soluble amorphous Ca phosphate, Al-IP, and Fe-IP into insoluble Ca-IP. Furthermore, compared to other pyrolysis temperatures, it was observed that the concentrations and percentages of Ca-IP had an obvious increase at 650 °C, demonstrating that the reaction temperature was an important factor for the effectiveness of the pyrolysis of animal manure. These consequences are in line with Huang et al.'s research study [39], which explained that a large portion of P in organic solid waste existed as phosphate species, probably in the form of mineral adsorbed species, phosphate minerals, and/or metal complexes; these species can experience phase transformations during oxygen-deficient heating processes: for example, the crystallization of amorphous phases and dewatering of hydrated phosphate minerals. Bruun et al. [40] also

verified that the pyrolysis of digested solids shows an obvious crystallization of calcium phosphate phases at temperatures beyond 600 °C.

### 3.2.6. OP

The percentages of OP highly decreased at 350 °C and then were kept invariable at higher temperatures (Figure 1F). These percentages of OP were 30.08%, 15.97%, and 34.22% in PM, CM, and SM, respectively; then, the percentages significantly decreased to 2.92% in PM800, 1.78% in CM800, and 4.66% in SM800 due to P transformations. The findings are in line with those originating from a previous research study, which showed that pyrolysis operations at 350 °C highly reduced the OP fraction by >61% in broiler litter and < 2% in cottonseed hull, observed in their biochar [41]. Xu et al. explained that pyrolysis could convert OP (NaHCO<sub>3</sub>-OP and NaOH-OP) into IP or other forms of stable organic P. The rapid decline in ortho-monoesters during pyrolysis revealed that OP in the mixture of wheat straw, maize straw, and peanut husk can decompose with ease at relatively low temperatures (>200 °C) and can be readily converted into IP (the two major constituent parts of the P pool: ortho-P and pyro-P) during pyrolysis [42]. Similar findings were also reported in a previous study that demonstrated the rapid decomposition of OP during pyrolysis [35]. The main forms of P in the three livestock manure types are SL-IP, Al-IP, and OP, accounting for 92.92% to 94.08% of the total P content. PM is the highest, and SM is the lowest. Then, the Olsen-P content was measured next.

### 3.3. Olsen-P

Olsen-P content is a reliable soil fertility indicator, and it is also a major factor that affects crop yields and that can be immediately absorbed by plants and microorganisms in soil [43]. It includes the vast majority of IP and a small part of OP, such as phosphate, phospholipids, DNA, and so on. The concentrations and rates of Olsen-P in PM, CM, SM, and the derived biochar are revealed in Table 4, respectively. The results show that the concentration of Olsen-P in SM (3.95 mg g<sup>-1</sup>) is lower than in PM (5.73 mg g<sup>-1</sup>), but the rate of Olsen-P relative to the total P in SM (49.67%) is higher than in PM (27.62%). Among them, Olsen-P content in CM was the highest. It is worth noting that the rates of Olsen-P relative to the total P in CMB decreased from 57.78% to 18.46% at 200–350 °C and then increased inconceivably from 23.9% to 38.05% at 650–800 °C, whereas those in PMB and SMB gradually reduced with an increase in pyrolysis temperature and decreased slowly when the pyrolysis temperature ranged between 650 and 800 °C (PMB, 3.4%–3.1%; SMB, 12.36%–9.65%). As mentioned above, the pyrolysis temperature at 650 °C was the preferred condition for the reduction in Olsen-P. From a different perspective, the derived biochar (PMB, CMB, and SMB) exhibited extensive pore structures, high cation exchange capacities, and high phosphate anion adsorbability, and these properties help improve soil fertility and the continuous release of Olsen-P if the derived biochar is applied to soil systems [44].

**Table 4.** Olsen-P content in manure and biochar.

	Manure	Biochar 200	Biochar 350	Biochar 500	Biochar 650	Biochar 800
PM	5.73 ± 0.25 <sup>a</sup>	4.94 ± 0.12 <sup>b</sup>	4.45 ± 0.23 <sup>c</sup>	5.02 ± 0.14 <sup>b</sup>	1.53 ± 0.13 <sup>d</sup>	1.38 ± 0.12 <sup>d</sup>
CM	7.93 ± 0.14 <sup>b</sup>	6.52 ± 0.24 <sup>c</sup>	4.89 ± 0.31 <sup>e</sup>	5.75 ± 0.10 <sup>d</sup>	7.71 ± 0.19 <sup>b</sup>	12.36 ± 0.37 <sup>a</sup>
SM	3.95 ± 0.14 <sup>b</sup>	3.43 ± 0.11 <sup>c</sup>	5.16 ± 0.13 <sup>a</sup>	5.03 ± 0.10 <sup>a</sup>	2.15 ± 0.11 <sup>d</sup>	1.73 ± 0.09 <sup>e</sup>
Proportion (%)	Manure	Biochar 200	Biochar 350	Biochar 500	Biochar 650	Biochar 800
PM	27.62 ± 1.83 <sup>a</sup>	21.19 ± 0.87 <sup>b</sup>	11.87 ± 0.78 <sup>c</sup>	11.64 ± 0.39 <sup>c</sup>	3.40 ± 0.23 <sup>d</sup>	3.10 ± 0.22 <sup>d</sup>
CM	57.78 ± 1.06 <sup>a</sup>	41.84 ± 0.98 <sup>b</sup>	18.46 ± 1.29 <sup>e</sup>	19.54 ± 0.59 <sup>e</sup>	23.90 ± 1.32 <sup>d</sup>	38.05 ± 1.56 <sup>c</sup>
SM	49.67 ± 1.42 <sup>a</sup>	38.67 ± 1.10 <sup>b</sup>	37.16 ± 1.70 <sup>b</sup>	31.49 ± 0.83 <sup>c</sup>	12.36 ± 0.98 <sup>d</sup>	9.65 ± 0.65 <sup>e</sup>

Date was reported as mean value ± SD. Different lowercase letters indicate significance ( $p < 0.05$ , Tukey's test) among materials and the derived biochar within the same material.

### 3.4. XRD of Raw Materials and the Derived Biochar of Olsen-P

The main phosphate compositions in PM, CM, SM, and their derived biochar were detected via XRD, and they are shown via characteristic XRD peaks in Figure 2. In this study,  $\text{AlPO}_4$ ,  $\text{K}_3\text{Al}_2(\text{PO}_4)_3$ , and  $\text{Al}_2(\text{PO}_4)(\text{OH})_3$  were the dominant phosphates in PM, CM, and SM, while stable phosphate crystals, such as calcium phosphate (Ca-P) and lead phosphate (Pb-P), were primarily observed in the derived biochar, indicating that pyrolysis was effective in the stabilization of P [45]. Additionally,  $\text{Ca}_8\text{Pb}_2(\text{PO}_4)_6(\text{OH})_2$  first appeared in CM650 and even SM800, whereas it was observed as early as in PM350 after pyrolysis; these results may be associated with the composition of raw materials [46]. Furthermore, the number of stable phosphate crystal species in the derived biochars increased with an increase in pyrolysis temperature. For example, there was only one type of Ca-P in CM200, but two types existed in CM350; then, three types existed in CM500 and CM650. The immobilization of P in the pyrolysis process is related to the pH, temperature, and concentration of Ca and P during the process [9], and pyrolysis temperatures need to exceed 500 °C preferably for the fixation of P of manure.

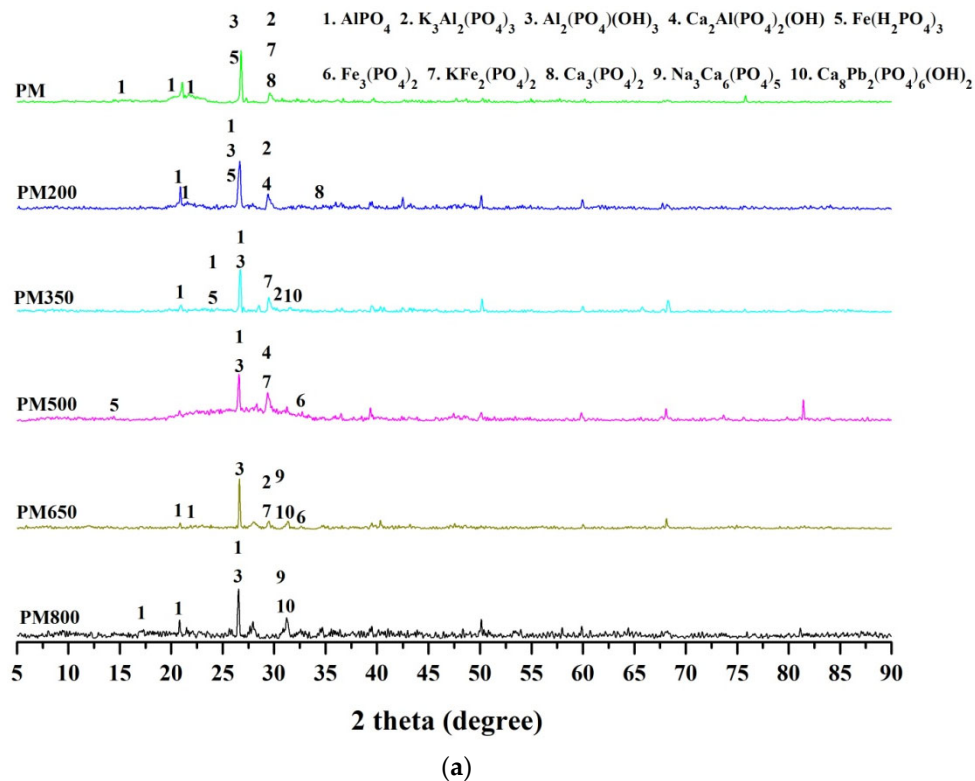
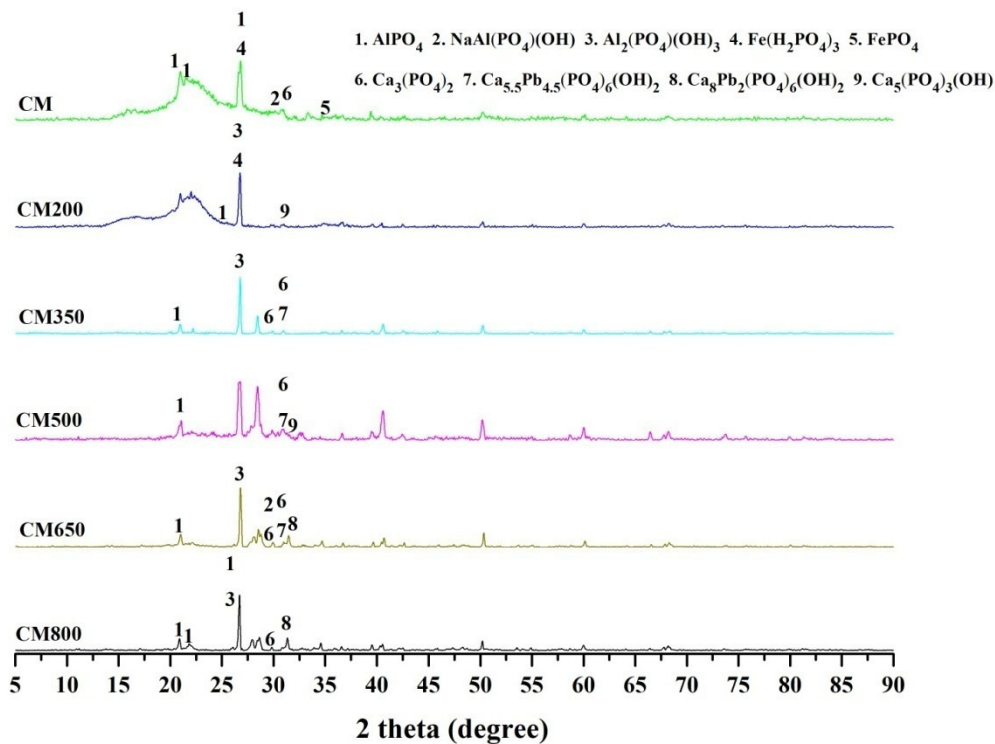
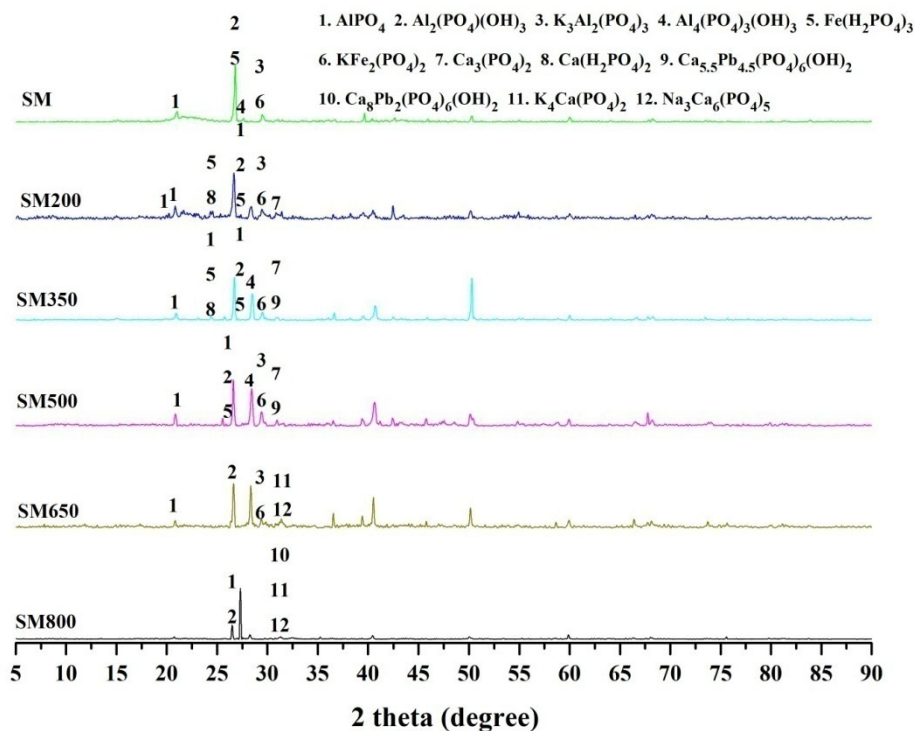


Figure 2. Cont.



(b)



(c)

**Figure 2.** X-ray diffraction patterns of (a) pig manure and the derived biochar, (b) cow manure and the derived biochar, and (c) sheep manure and the derived biochar.

#### 4. Conclusions

A comprehensive exploration of P forms in PM, CM, and SM and their derived biochar can contribute to an improved evaluation of the quantity of P, which would be helpful for crop growth and water eutrophication reduction. In this study, total P

content analysis revealed that high P concentrations existed in three types of manure, and more than 92% of P was concentrated in the derived biochar during pyrolysis processes carried out at 200–800 °C. The P speciation analysis also showed that SL-IP, AI-IP, and OP transformed into more stable P fractions such as Ca-IP and O-IP after pyrolysis; in particular, the percentages of Ca-IP in PMB800 reached 79.01%. XRD also demonstrated that calcium phosphate (Ca-P) and lead phosphate (Pb-P) were primarily observed in the derived biochar after pyrolysis processes, and more species of stable phosphate crystals were observed in the derived biochar. The Olsen-P percentages decreased after pyrolysis at temperatures of 200–800 °C and were distinctly reduced from 500 °C to 650 °C, indicating that pyrolysis at 650 °C was the optimal condition for the reduction in Olsen-P content in manure. In summary, pyrolysis is an effective treatment method for P immobilization in PM, CM, and SM, and this study lays the foundation for the assessment of P recyclability in animal manure.

**Author Contributions:** F.L. formulated the research plan, analyzed the data, wrote the original draft, and finalized the research paper. Z.X. and J.F. designed the research, highlighted the problem, reviewed the draft paper, and financially supported the article. H.L. helped in the development and analysis of results. All authors have read and agreed to the published version of the manuscript.

**Funding:** This research was funded by the Hunan Provincial Science and Technology Department Project (2020NK2004, 2021JJ30008) and the Key Project Science Foundation of Hunan Education Department, China (S202210537011).

**Data Availability Statement:** Data will be made available on request.

**Acknowledgments:** The authors are thankful to the Hunan Engineering Laboratory for Pollution Control and Waste Utilization in Swine Production, Hunan Agricultural University, Changsha, and the Key Laboratory for Rural Ecosystem Health in Dongting Lake Area of Hunan Province, Changsha, for providing the experimental condition to this article. The authors would also like to extend their gratitude to the reviewers and editorial office for their comments and for improving the quality of the manuscript.

**Conflicts of Interest:** The authors declare no conflict of interest.

## References

1. Wang, Y.; Zhang, Y.; Li, J.; Lin, J.-G.; Zhang, N.; Cao, W. Biogas Energy Generated from Livestock Manure in China: Current Situation and Future Trends. *J. Environ. Manag.* **2021**, *297*, 113324. [[CrossRef](#)] [[PubMed](#)]
2. Li, L.; Zou, D.; Xiao, Z.; Zeng, X.; Zhang, L.; Jiang, L.; Wang, A.; Ge, D.; Zhang, G.; Liu, F. Biochar as a Sorbent for Emerging Contaminants Enables Improvements in Waste Management and Sustainable Resource Use. *J. Clean. Prod.* **2019**, *210*, 1324–1342. [[CrossRef](#)]
3. Zeng, X.; Zou, D.; Wang, A.; Zhou, Y.; Liu, Y.; Li, Z.; Liu, F.; Wang, H.; Zeng, Q.; Xiao, Z. Remediation of Cadmium-Contaminated Soils Using Brassica Napus: Effect of Nitrogen Fertilizers. *J. Environ. Manag.* **2020**, *255*, 109885. [[CrossRef](#)] [[PubMed](#)]
4. Dalu, T.; Wasserman, R.J.; Magoro, M.L.; Froneman, P.W.; Weyl, O.L.F. River Nutrient Water and Sediment Measurements Inform on Nutrient Retention, with Implications for Eutrophication. *Sci. Total Environ.* **2019**, *684*, 296–302. [[CrossRef](#)]
5. Wan, W.; Wang, Y.; Tan, J.; Qin, Y.; Zuo, W.; Wu, H.; He, H.; He, D. Alkaline Phosphatase-Harboring Bacterial Community and Multiple Enzyme Activity Contribute to Phosphorus Transformation during Vegetable Waste and Chicken Manure Composting. *Bioresour. Technol.* **2020**, *297*, 122406. [[CrossRef](#)] [[PubMed](#)]
6. Xu, F.; Ma, H.; Liang, J.; Okopi, S.I.; Yang, S.; Cao, L.; Sun, W. Effects of Different Conditions Tested “in Vitro” on the Phosphorus Runoff Potential of Livestock Manure. *Waste Manag.* **2022**, *147*, 30–35. [[CrossRef](#)] [[PubMed](#)]
7. Adhikari, S.; Gascó, G.; Méndez, A.; Surapaneni, A.; Jegatheesan, V.; Shah, K.; Paz-Ferreiro, J. Influence of Pyrolysis Parameters on Phosphorus Fractions of Biosolids Derived Biochar. *Sci. Total Environ.* **2019**, *695*, 133846. [[CrossRef](#)]
8. Zhang, W.; Tang, X.; Feng, X.; Wang, E.; Li, H.; Shen, J.; Zhang, F. Management Strategies to Optimize Soil Phosphorus Utilization and Alleviate Environmental Risk in China. *J. Environ. Qual.* **2019**, *48*, 1167–1175. [[CrossRef](#)] [[PubMed](#)]
9. Li, B.; Dinkler, K.; Zhao, N.; Sobhi, M.; Merkle, W.; Liu, S.; Dong, R.; Oechsner, H.; Guo, J. Influence of Anaerobic Digestion on the Labile Phosphorus in Pig, Chicken, and Dairy Manure. *Sci. Total Environ.* **2020**, *737*, 140234. [[CrossRef](#)]
10. Yang, Y.; Meehan, B.; Shah, K.; Surapaneni, A.; Hughes, J.; Fouché, L.; Paz-Ferreiro, J. Physicochemical Properties of Biochars Produced from Biosolids in Victoria, Australia. *Int. J. Environ. Res. Public Health* **2018**, *15*, 1459. [[CrossRef](#)] [[PubMed](#)]
11. Zhang, T.; He, X.; Deng, Y.; Tsang, D.C.W.; Yuan, H.; Shen, J.; Zhang, S. Swine Manure Valorization for Phosphorus and Nitrogen Recovery by Catalytic-Thermal Hydrolysis and Struvite Crystallization. *Sci. Total Environ.* **2020**, *729*, 138999. [[CrossRef](#)] [[PubMed](#)]

12. Jiang, Y.; Ren, C.; Guo, H.; Guo, M.; Li, W. Speciation Transformation of Phosphorus in Poultry Litter during Pyrolysis: Insights from X-Ray Diffraction, Fourier Transform Infrared, and Solid-State NMR Spectroscopy. *Environ. Sci. Technol.* **2019**, *53*, 13841–13849. [[CrossRef](#)]
13. Cui, X.; Yang, X.; Sheng, K.; He, Z.; Chen, G. Transformation of Phosphorus in Wetland Biomass during Pyrolysis and Hydrothermal Treatment. *ACS Sustain. Chem. Eng.* **2019**, *7*, 16520–16528. [[CrossRef](#)]
14. Chen, X.; Gao, M.; Li, Y.; Zhang, X.; Zhang, F.; Hu, B. Effects of Freeze-Thaw Cycles on the Physicochemical Characteristics of Animal Manure and Its Phosphorus Forms. *Waste Manag.* **2019**, *88*, 160–169. [[CrossRef](#)] [[PubMed](#)]
15. Zhang, X.; Lin, H.; Wei, W.; Hu, B. Electrocoagulation of Dairy Manure Using Low-Carbon Steel Electrodes for Phosphorus Removal. *J. Environ. Eng.* **2020**, *146*, 04020044. [[CrossRef](#)]
16. Liu, L.; Tan, Z.; Gong, H.; Huang, Q. Migration and Transformation Mechanisms of Nutrient Elements (N, P, K) within Biochar in Straw–Biochar–Soil–Plant Systems: A Review. *ACS Sustain. Chem. Eng.* **2019**, *7*, 22–32. [[CrossRef](#)]
17. Sánchez-García, M.; Cayuela, M.L.; Rasse, D.P.; Sánchez-Monedero, M.A. Biochars from Mediterranean Agroindustry Residues: Physicochemical Properties Relevant for C Sequestration and Soil Water Retention. *ACS Sustain. Chem. Eng.* **2019**, *7*, 4724–4733. [[CrossRef](#)]
18. Fang, Z.; Liu, F.; Li, Y.; Li, B.; Yang, T.; Li, R. Influence of Microwave-Assisted Pyrolysis Parameters and Additives on Phosphorus Speciation and Transformation in Phosphorus-Enriched Biochar Derived from Municipal Sewage Sludge. *J. Clean. Prod.* **2021**, *287*, 125550. [[CrossRef](#)]
19. Zhao, Z.; Wang, B.; Zhang, X.; Xu, H.; Cheng, N.; Feng, Q.; Zhao, R.; Gao, Y.; Wei, M. Release Characteristics of Phosphate from Ball-Milled Biochar and Its Potential Effects on Plant Growth. *Sci. Total Environ.* **2022**, *821*, 153256. [[CrossRef](#)] [[PubMed](#)]
20. Chu, G.; Wang, W.; Zhao, J.; Zhou, D. Transformation of Phosphorus Species during Phosphoric Acid-Assisted Pyrolysis of Lignocellulose. *Sci. Total Environ.* **2023**, *866*, 161010. [[CrossRef](#)] [[PubMed](#)]
21. Li, M.; Tang, Y.; Lu, X.-Y.; Zhang, Z.; Cao, Y. Phosphorus Speciation in Sewage Sludge and the Sludge-Derived Biochar by a Combination of Experimental Methods and Theoretical Simulation. *Water Res.* **2018**, *140*, 90–99. [[CrossRef](#)] [[PubMed](#)]
22. Zhu, Y.; Zhao, Q.; Li, D.; Li, J.; Guo, W. Performance Comparison of Phosphorus Recovery from Different Sludges in Sewage Treatment Plants through Pyrolysis. *J. Clean. Prod.* **2022**, *372*, 133728. [[CrossRef](#)]
23. Backnäs, S.; Laine-Kaulio, H.; Kløve, B. Phosphorus Forms and Related Soil Chemistry in Preferential Flowpaths and the Soil Matrix of a Forested Podzolic till Soil Profile. *Geoderma* **2012**, *189–190*, 50–64. [[CrossRef](#)]
24. Müller, A.L.; Reichmann, W. *Architecture, Materiality and Society*; Palgrave Macmillan UK: London, UK, 2015; Volume 27, ISBN 978-1-349-69001-5.
25. Shen, J.; Li, R.; Zhang, F.; Fan, J.; Tang, C.; Rengel, Z. Crop Yields, Soil Fertility and Phosphorus Fractions in Response to Long-Term Fertilization under the Rice Monoculture System on a Calcareous Soil. *Field Crops Res.* **2004**, *86*, 225–238. [[CrossRef](#)]
26. Szögi, A.A.; Vanotti, M.B.; Hunt, P.G. Phosphorus Recovery from Pig Manure Solids Prior to Land Application. *J. Environ. Manag.* **2015**, *157*, 1–7. [[CrossRef](#)]
27. Huang, R.; Fang, C.; Zhang, B.; Tang, Y. Transformations of Phosphorus Speciation during (Hydro)Thermal Treatments of Animal Manures. *Environ. Sci. Technol.* **2018**, *52*, 3016–3026. [[CrossRef](#)]
28. Mickdam, E.; Khiaosa-ard, R.; Metzler-Zebeli, B.U.; Humer, E.; Harder, H.; Khol-Parisini, A.; Zebeli, Q. Modulation of Ruminant Fermentation Profile and Microbial Abundance in Cows Fed Diets Treated with Lactic Acid, without or with Inorganic Phosphorus Supplementation. *Anim. Feed Sci. Technol.* **2017**, *230*, 1–12. [[CrossRef](#)]
29. Yu, Z.; Jin, J.; Hou, F.; Zhang, Y.; Wang, G.; Liu, B.; Zhai, Z. Understanding Effect of Phosphorus-Based Additive on Ash Deposition Characteristics during High-Sodium and High-Calcium Zhundong Coal Combustion in Drop-Tube Furnace. *Fuel* **2021**, *287*, 119462. [[CrossRef](#)]
30. Liu, L.; Guo, Y.; Tu, Y.; Zhang, N.; Bai, Z.; Chadwick, D.; Dou, Z.; Ma, L. A Higher Water-Soluble Phosphorus Supplement in Pig Diet Improves the Whole System Phosphorus Use Efficiency. *J. Clean. Prod.* **2020**, *272*, 122586. [[CrossRef](#)]
31. Bindraban, P.S.; Dimkpa, C.O.; Pandey, R. Exploring Phosphorus Fertilizers and Fertilization Strategies for Improved Human and Environmental Health. *Biol. Fertil. Soils* **2020**, *56*, 299–317. [[CrossRef](#)]
32. Hedley, M.; McLaughlin, M. Reactions of Phosphate Fertilizers and By-Products in Soils. *Phosphorus Agric. Environ.* **2015**, *46*, 181–252.
33. Chahine, S.; Garau, G.; Castaldi, P.; Vittoria, M.; Sara, P.; Seddaiu, G.; Roggero, P.P. Stabilising Fluoride in Contaminated Soils with Monocalcium Phosphate and Municipal Solid Waste Compost: Microbial, Biochemical and Plant Growth Impact. *Environ. Sci. Pollut. Res.* **2022**, *29*, 41820–41833. [[CrossRef](#)] [[PubMed](#)]
34. Haque, S.E. How Effective Are Existing Phosphorus Management Strategies in Mitigating Surface Water Quality Problems in the U.S.? *Sustainability* **2021**, *13*, 6565. [[CrossRef](#)]
35. Qian, T.; Jiang, H. Migration of Phosphorus in Sewage Sludge during Different Thermal Treatment Processes. *Sustain. Chem. Eng.* **2014**, *2*, 1411–1419. [[CrossRef](#)]
36. Timofeeva, A.; Galyamova, M.; Sedykh, S. Prospects for Using Phosphate-Solubilizing Microorganisms as Natural Fertilizers in Agriculture. *Plants* **2022**, *11*, 2119. [[CrossRef](#)] [[PubMed](#)]
37. Eduah, J.O.; Nartey, E.K.; Abekoe, M.K.; Breuning-madsen, H.; Andersen, M.N. Geoderma Phosphorus Retention and Availability in Three Contrasting Soils Amended with Rice Husk and Corn Cob Biochar at Varying Pyrolysis Temperatures. *Geoderma* **2019**, *341*, 10–17. [[CrossRef](#)]

38. Yuan, H.; Tai, Z.; Li, Q.; Liu, E. In-situ, high-resolution evidence from water-sediment interface for significant role of iron bound phosphorus in eutrophic lake. *Sci. Total Environ.* **2019**, *706*, 136040. [[CrossRef](#)] [[PubMed](#)]
39. Huang, R.; Fang, C.; Lu, X.; Jiang, R.; Tang, Y. Transformation of Phosphorus during (Hydro)Thermal Treatments of Solid Biowastes: Reaction Mechanisms and Implications for P Reclamation and Recycling. *Environ. Sci. Technol.* **2017**, *51*, 10284–10298. [[CrossRef](#)] [[PubMed](#)]
40. Bruun, S.; Harmer, S.L.; Bekiaris, G.; Christel, W.; Zuin, L.; Hu, Y.; Jensen, L.S.; Lombi, E. The Effect of Different Pyrolysis Temperatures on the Speciation and Availability in Soil of P in Biochar Produced from the Solid Fraction of Manure. *Chemosphere* **2017**, *169*, 377–386. [[CrossRef](#)]
41. Uchimiya, M.; Hiradate, S. Pyrolysis Temperature-Dependent Changes in Dissolved Phosphorus Speciation of Plant and Manure Biochars. *J. Agric. Food Chem.* **2014**, *62*, 1802–1809. [[CrossRef](#)] [[PubMed](#)]
42. Xu, G.; Zhang, Y.; Shao, H.; Sun, J. Pyrolysis Temperature Affects Phosphorus Transformation in Biochar: Chemical Fractionation and <sup>31</sup>P NMR Analysis. *Sci. Total Environ.* **2016**, *569–570*, 65–72. [[CrossRef](#)] [[PubMed](#)]
43. Wu, Q.; Zhang, S.; Feng, G.; Zhu, P.; Huang, S.; Wang, B.; Xu, M. Determining the Optimum Range of Soil Olsen P for High P Use Efficiency, Crop Yield, and Soil Fertility in Three Typical Cropland Soils. *Pedosphere* **2020**, *30*, 832–843. [[CrossRef](#)]
44. Wu, L.; Wei, C.; Zhang, S.; Wang, Y.; Kuzyakov, Y.; Ding, X. MgO-Modified Biochar Increases Phosphate Retention and Rice Yields in Saline-Alkaline Soil. *J. Clean. Prod.* **2019**, *235*, 901–909. [[CrossRef](#)]
45. Fang, J.; Liu, Z.; Luan, H.; Liu, F.; Yuan, X.; Long, S.; Wang, A.; Ma, Y.; Xiao, Z. Thermochemical Liquefaction of Cattle Manure Using Ethanol as Solvent: Effects of Temperature on Bio-Oil Yields and Chemical Compositions. *Renew. Energy* **2021**, *167*, 32–41. [[CrossRef](#)]
46. Luan, H.; Liu, F.; Long, S.; Liu, Z.; Qi, Y.; Xiao, Z.; Fang, J. The Migration, Transformation, and Risk Assessment of Heavy Metals in Residue and Bio-Oil Obtained by the Liquefaction of Pig Manure. *Environ. Sci. Pollut. Res.* **2020**, *28*, 15055–15069. [[CrossRef](#)] [[PubMed](#)]

**Disclaimer/Publisher’s Note:** The statements, opinions and data contained in all publications are solely those of the individual author(s) and contributor(s) and not of MDPI and/or the editor(s). MDPI and/or the editor(s) disclaim responsibility for any injury to people or property resulting from any ideas, methods, instructions or products referred to in the content.